MNRAS **000**, 1–5 (2016) Preprint 21 September 2016 Compiled using MNRAS LATEX style file v3.0

Discovery of an extended source of gamma-ray emission in the Southern hemisphere

Miguel Araya[1⋆]
[1]*Escuela de Física, Universidad de Costa Rica*

Accepted XXX. Received YYY; in original form ZZZ

arXiv:1609.06225v1 [astro-ph.HE] 20 Sep 2016

ABSTRACT

The discovery of a $\sim 3.^\circ4$-wide region of high-energy emission in data from the Fermi LAT satellite is reported. The region is located in the Southern hemisphere and relatively far from the plane of the Galaxy, around the Galactic coordinates l=350.6, b=-4.7. It shows a hard spectrum that is compatible with a power-law, $\frac{dN}{dE} \propto E^{-\Gamma}$, with a spectral index $\Gamma = 1.68 \pm 0.04_{\rm stat}$ above 200 MeV and a total integrated flux above 1 GeV of $(3.76 \pm 0.33_{\rm stat}) \times 10^{-9}$ cm^{-2} s^{-1}. Two hypotheses about the nature of the source are discussed, namely that the emission comes from the shell of an unknown supernova remnant or from a pulsar wind nebula.

Key words: cosmic rays – ISM: supernova remnants – gamma-rays: general – gamma-rays: ISM

1 INTRODUCTION

The current generation of gamma-ray observatories have revealed a large variety of Galactic and extragalactic sources of high-energy (MeV to GeV) and very high-energy (TeV) emission. In particular the all-sky survey of the *Fermi* Large Area Telescope (LAT) (Atwood et al. 2009) has had considerable impact in the science of high-energy astrophysics. Gamma-ray emitting objects observed by the LAT include supernova remnants (SNRs) and their surroundings, pulsar wind nebulae (PWN) and pulsars, binary systems, novae and supermassive black holes (e.g., Abdo et al. 2010b; Acero et al. 2013; Abdo et al. 2010a, 2009a; Ackermann et al. 2014a, 2015).

The origin of gamma-ray emission in all these systems is important to understand the physical processes behind the acceleration of particles. Its study may also help reveal the origin of Galactic cosmic rays. Several SNRs have been established as sources of high-energy protons (or nuclei) (e.g., Ackermann et al. 2013) but the search for the Galactic PeVatron continues and many of the observed sources remain unidentified.

SNRs also show a variety of spectra and features that are not fully understood, which points to the need for more studies and theoretical work on the problem of particle acceleration and transport (e.g., Abdo et al. 2009b; Yuan et al. 2011; Caprioli 2012; Bell 2014; Acero et al. 2016).

Many known Galactic extended sources at GeV and TeV energies are likely PWN or SNRs (Acero et al. 2015; Carrigan et al. 2013). Well studied examples of SNR shells that emit gamma-rays are RX J1713.7-3946 (Abdo et al. 2011) and RX J0852.0-4622 (Tanaka et al. 2011). These sources show a hard GeV spectrum which can be explained by inverse Compton (IC) scattering of soft photons by high-energy leptons, although the origin of the emission is still debated. Also, most of these sources are found close to the Galactic equator, which is expected since gamma-ray sources are related to young stellar populations. A notable exception is the unidentified source HESS J1507-622 (H.E.S.S. Collaboration et al. 2011) which lies about $3^\circ.5$ from the plane of the Galaxy and has no clear X-ray counterpart, which is surprising given the low absorption expected at its location. This also prevents for a clear determination of its distance, a key parameter to understand its nature. It has been suggested that this and other unidentified gamma-ray sources could be ancient PWN with no counterpart at other wavelengths (Vorster et al. 2013).

Here, the discovery of an extended source of gamma-rays seen in LAT data is reported. The source shows a hard photon spectrum. When modeled with a uniform disc template, the center of the emission is located at the Galactic coordinates $l = 350.^\circ6$, $b = -4.^\circ7$ and its best-fit radius is $1.^\circ7$. Several gamma-ray sources have been found in the region previously. In the latest *Fermi* LAT catalog (Acero et al. 2015), the unidentified sources 3FGL J1733.5-3941 and 3FGL J1748.5-3912 lie close to the boundary of the new source, although according to the catalog they show a softer spectrum. The source 3FGL J1747.6-4037 is also near the boundary of the new extended source and it is identified as the gamma-ray counterpart of the millisecond pulsar PSR J1747-4036 with a dispersion measure that implies a source distance of 3.4 kpc and its spindown luminosity is 1.16×10^{35}

⋆ E-mail: miguel.araya@ucr.ac.cr

© 2016 The Authors

erg s^{-1} (uncorrected for the Shklovskii effect) (Kerr et al. 2012; Abdo et al. 2013). It is a faint gamma-ray pulsar and its spectral curvature could not be seen with three years of LAT data. The unidentified point-like source 2FHL J1741.2-4021, discovered with the LAT and reported in the Second *Fermi* LAT Catalog of High-Energy Sources (Ackermann et al. 2016) for sources detected above 50 GeV, is found within the extended new region. Finally, no SNRs or PWN are known within the extent of the region.

In this paper, the data selection, analysis and results are described in Section 2. In Section 3 possible interpretations of the nature of this source are given.

2 DATA ANALYSIS

Fermi LAT data were gathered from 2008 August to 2016 September from the LAT data server[1]. The most recent photon and spacecraft data release (PASS 8) were used to process the data, which shows improvements with respect to previous releases in event reconstructions, increased effective area and better energy measurements. The instrument response functions used are P8R2_SOURCE_V6 and data were analyzed with the public Science Tools software for LAT data, version v10r0p5. Recommended cuts for standard analysis are applied which include selecting SOURCE class events and a maximum zenith angle selection of 90° to avoid albedo gamma rays from the Earth, time intervals when the data quality is good and the data taking mode is standard.

A 20° × 20° region of interest, centered at the coordinates RA=264.°86, Dec=-39.°5, is used in the analysis with events having energies between 200 MeV and 500 GeV. The data is binned spatially in counts maps with a scale of 0.°05 per pixel and using ten logarithmically spaced bins per decade in energy for exposure calculation. The analysis includes sources from the most recent LAT catalog (3FGL) and the standard galactic diffuse emission model (described by the file gll_iem_v06.fits) and the isotropic component (iso_P8R2_SOURCE_V6_v06.txt) distributed with the LAT analysis software.

The spectral and morphological properties of sources are studied with a maximum likelihood analysis (Mattox et al. 1996) during which the normalizations of the diffuse components are left free in the fit. The significance for the detection of a source is estimated as the square root of the test statistic (TS), which is defined as $-2\times\log(L_0/L)$, where L_0 is the likelihood value without the source and L the likelihood with the additional source.

2.1 Morphology of the emission

In order to take advantage of the narrower LAT point-spread function at higher energies the region is first examined above 5 GeV to study the morphology of the emission. The model for the region is constructed as described above and a maximum likelihood fit is performed. If a source is not detected above this energy, the value of its spectral parameters are kept fixed, except for the source 3FGL J1733.5-3941 which, being so close to the region studied, will have its spectral parameters fixed at the values found above 5 GeV to facilitate convergence of the fits done when studying the nearby extended emission.

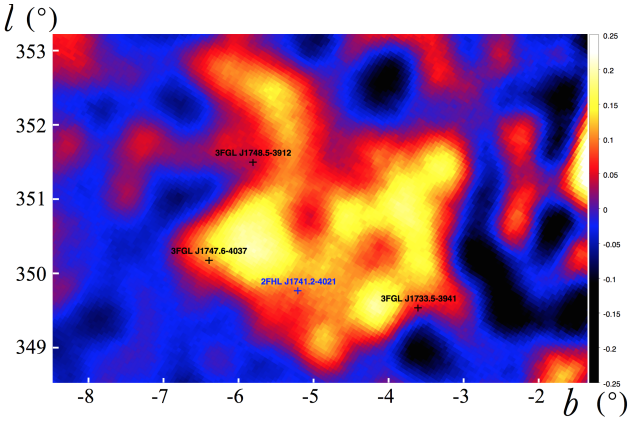

Figure 1. LAT counts map above 5 GeV obtained after subtraction of the background model. The image is smoothed with a 0.°5 wide Gaussian kernel. The positions of sources found in the latest LAT catalog (3FGL), which are included in the model, and a source present in the high-energy catalog (>50 GeV, 2FHL), which is not included in the model, are labeled. The source 3FGL J1747.6-4037 is the gamma-ray counterpart of the pulsar mentioned in the text while the other sources are unidentified.

After the initial fit, a template for the backgound model is created which is then subtracted from the observed counts map. The map of the residual emission near the area of interest is shown in Fig. 1 in Galactic coordinates. A several degree-wide region of emission is seen in the image.

In order to study the morphology of the emission, the region is modeled with two spatial hypotheses: a uniform disc and a collection of point sources. The spectra used in all cases is a simple power law. The disc template is placed within the interior of the region and its center position is moved in a 1° × 1° square grid with the origin at the coordinates RA=284.°86, Dec=-39.°5, in steps of 0.°1, changing sistematically its radius at each position in steps of 0.°1 from 0.5 to 2.0 degrees, while at the same time fitting the spectral normalization and index to find the maximum likelihood.

The point sources used in the point-source hypothesis are placed at the positions of maximum excess seen in Fig. 1. Individual point sources are considered as part of the final best-fit template whenever their individual TS values are greater than three. The results of the fits with the two spatial hypotheses are shown in Table 1.

As can be seen in Table 1, the uniform disc model is preferred since the extended emission hypothesis shows a TS∼137 above 5 GeV. The bes-fit template is centered at the Galactic coordinates $(l, b) = 350.°63, -4.°71$ and has a radius of $1.°7 \pm 0.°2$. The 3-σ uncertainty in the position is 0.°3 and was estimated from the change in the source TS resulting from displacing the disc from the best-fit position. The gamma-ray source is thus referred to as G350.6-4.7 from now on.

It is noted that a different spatial hypothesis containing several independent and extended sources in the region is not tested here, and this is left for a future work. Confusion

[1] See http://fermi.gsfc.nasa.gov

Table 1. Likelihood results for different hypotheses for the morphology of the emission.

Spatial model	TS†
Best-fit disc template	137.5
2 point sources	14
3 point sources	89
4 point sources	73

†Test statistic compared with the null hypothesis of no gamma-ray emission.

of several extended sources might be possible although this probably becomes less likely the farther this region actually is from the Galactic plane as source populations drop.

2.2 Additional gamma-ray background in the region

In order to probe for additional gamma-ray emission that might be present in the region around the source G350.6-4.7 and which is not accounted for in the model, a uniform disc template of radius 1.°7 is moved through different positions around the excess seen in Fig. 1 and a likelihood fit is performed above 5 GeV without including the template for the source G350.6-4.7. The significance and spectral index of any nearby extended excess is then estimated.

No significant extended gamma-ray emission around G350.6-4.7 is detected.

Possible residual gamma-ray emission is also probed in this way in a $10^\circ \times 10^\circ$ region around the coordinates RA=272°, Dec=-34° towards the Galactic Center region. The region around G350.6-4.7 is located well within the "Fermi bubbles", a pair of extended structures seen in gamma-rays by the *Fermi* satellite (Su et al. 2010). It has been found later that a simple power law spectrum is not consistent with the spectrum of the bubbles, which instead show a spectrum above 1 GeV which is consistent with a power-law with an exponential cutoff with index ~ 1.87 and a cutoff energy of ~ 113 GeV (Ackermann et al. 2014b).

No significant additional background emission is detected towards the Galactic center. Although a template for the Fermi bubbles is included in the background for all the analysis presented here according to the standard analysis of LAT data, it is possible that the bubbles show additional structure that is not accounted for by this template. However, based on the spectral results from Section 2.3, it can be stated that the spectrum of G350.6-4.7 is different from that of the bubbles.

2.3 Spectrum

The best-fit spatial template found in Section 2.1 is now used to obtain the source spectrum above 200 MeV. In order to probe for curvarture in the spectrum different spectral shapes are used in independent likelihood fits: a simple power law and a log parabola. The TS values obtained for each spectral assumption are, respectively, 246 and 247 for an additional degree of freedom in the curved spectrum. These results imply that the best-fit spectral shape is a simple power law and thus the source shows no spectral curvature in the LAT energy range.

Above 200 MeV the best-fit power-law ($\frac{dN}{dE} \propto E^{-\Gamma}$) index is $1.68 \pm 0.04_{\rm stat}$ and the integrated flux above 1 GeV is $(3.76 \pm 0.33_{\rm stat}) \times 10^{-9}$ cm^{-2} s^{-1}. The source detection significance above 200 MeV is thus 15σ.

In agreement with the results from this Section, that there is no spectral curvature in the LAT energy range, the overall spectral slope above 200 MeV is very similar to the one found in the morphological analysis above 5GeV.

3 DISCUSSION

The morphological analysis of Section 2.1 implies that, when modeled as a uniform disc, the gamma-ray emission from the source G350.6-4.7 has an intrinsic diameter of $\sim 3^\circ.4$. Possible interpretations of the origin of the emission are now discussed.

It is reasonable to assume that the gamma-rays come from the shell of a previously unknown SNR. If located at the distance of the pulsar PSR J1747-4036 (3.4 kpc) the object size would be around 200 pc and the center of the disc would be located around 250 pc from the plane of the Galaxy. SNRs with diameters of the order of a few degrees are known and some have been seen as extended objects by the LAT (for example, the Cygnus Loop, Katagiri et al. (2011) and RX J0852.0-4622, Tanaka et al. (2011)), but most of the large angular diameter SNRs are located within 0.3-2 kpc from Earth.

From dynamic considerations of the expansion and evolution of a SNR (e.g., Cioffi et al. 1988; Slavin & Cox 1993) and the fact that not many SNRs are known to have a diameter greater than 100 pc it is likely that this new source is much closer than 3.4 kpc and hence unrelated to PSR J1747-4036. The Cygnus Loop is located at about 540 pc (Blair et al. 2005) and has a diameter of $\sim$ 35 pc. If the same physical diameter is assumed for G350.6-4.7, the resulting distance would be similar. However, the LAT spectrum of the Cygnus Loop (Katagiri et al. 2011) is quite different to that reported here for G350.6-4.7 so these two objects might have very different properties. On the other hand, with a diameter of $\sim 2^\circ$ (or $\sim$26 pc), RX J0852.0-4622 shows a GeV spectrum that is similar in shape to that of G350.6-4.7 (Tanaka et al. 2011). Both of these SNRs, however, have very clear counterparts at other wavelengths.

There are candidate SNR shells that are detected at TeV energies and have no known counterparts at other wavelengths, such as HESS J1912+101 (Pühlhofer et al. 2015). A preliminary analysis done here for LAT data at this source position reveals several GeV hotspots whose soft spectra do not seem to be compatible with the spectrum of the TeV source and thus might be unrelated to it. It is possible that G350.6-4.7 is an example of this kind of TeV shells, except that the LAT telescope in this case is able to observe the

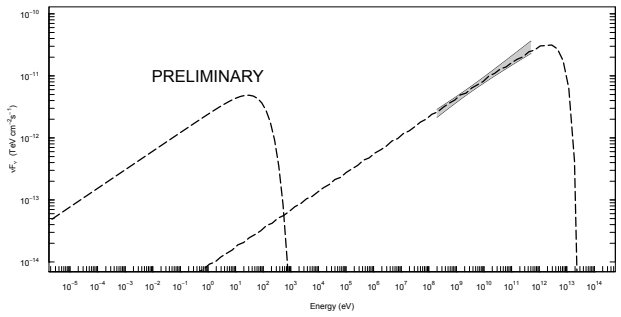

Figure 2. The spectral energy distribution of G350.6-4.7 is shown here above 200 MeV. The shaded region represents the 1σ fit uncertainty and the dashed lines are the simple leptonic model described in the text.

hard GeV spectrum. Follow up radio, X-ray and TeV observations of G350.6-4.7 are necessary to understand its nature.

It might be natural to assume from the spectral shape of G350.6-4.7 that the gamma-rays are produced by IC scattering of high-energy electrons. Fig. 2 shows the SED of the source with a leptonic model. The particle distribution is a power-law with a cutoff in energy of the form $\frac{dN_e}{d\epsilon} \propto \epsilon^{-s} \cdot \mathrm{e}^{-\epsilon/\epsilon_c}$ with $\epsilon_c = 35$ TeV and spectral index $s = 2.4$. The particles are assumed to be uniformly distributed in a spherical volume of radius 15 pc located 500 pc away and the total particle energy is 1.9×10^{49} erg. If G350.6-4.7 is located significantly away from the Galactic plane, the dominant photon field to serve as seed for upscattering is the CMB, which is used here. The magnetic field value used is 1 μG.

The particle cutoff energy is of course not constrained by the LAT data. For the value used here, the peak of the synchrotron spectral energy distribution would be seen at a photon energy of 20 eV. The inverse Compton scattering cooling time of a high-energy lepton with Lorentz factor $\gamma = 7 \times 10^7$ interacting with the CMB is given by (Longair 1994)

$$\tau = \frac{\epsilon}{\frac{4}{3}\sigma_T c \gamma^2 U_{\mathrm{CMB}}} = \frac{2.3 \times 10^{12}\ \mathrm{yr}}{\gamma} \approx 33\ \mathrm{kyr}. \quad (1)$$

If the source age is lower than a few kyr it is likely that it could be detected at TeV energies in this scenario.

In this scenario, the electron energy density at the source would be 28 eV/cm^3.

Another scenario for the origin of the gamma-rays is the hadronic emission from cosmic rays in the shell of a SNR. The hadronic gamma ray flux above a photon energy of 1 GeV from a SNR located at a distance d is given by (Drury et al. 1994)

$$F \approx 1.8{\times}10^{-7}\,\theta \left(\frac{E_{\mathrm{SN}}}{10^{51}\,\mathrm{erg}}\right) \left(\frac{d}{1\,\mathrm{kpc}}\right)^{-2} \left(\frac{n}{1\,\mathrm{cm}^{-3}}\right)\ \mathrm{cm}^{-2}\,\mathrm{s}^{-1}, \quad (2)$$

assuming a cosmic-ray distribution close to that resulting from test-particle diffusive shock acceleration. Here, $\theta \sim 0.1$ is the fraction of the total supernova explosion energy ($E_{\mathrm{SN}} = 10^{51}$ erg) converted to cosmic ray energy and n the ambient density. Using these values and the measured flux this translates to $n_1/d_1^2 \approx 0.21$, where the distance d_1 is in units of 1 kpc and the ambient density n_1 in units of cm^{-3}. For $d_1 = 0.5$ this implies $n_1 = 0.05$.

Galactic gas distribution models and constraints on the cosmic ray energetics for off-plane gamma ray sources such as HESS J1507-622 (Domainko 2011), located 3.°5 away from the plane of the Galaxy, predict an ambient density of $n_1 \sim 0.55$ for a source distance of 500 pc. The hadronic scenario for G350.6-4.7 is therefore plausible for $d = 500$ pc. For a source distance of 2 kpc the required density is $n_1 \sim 0.8$ which might be high for an off-plane distance of 160 pc (Domainko 2011). In a hadronic scenario, the source distance is likely < 2 kpc, although this of course would change for a more energetic progenitor SN event or a different cosmic-ray acceleration efficiency.

The 70 Month Swift-BAT All-sky Hard X-Ray Survey (Baumgartner et al. 2013) with a flux limit of 1.3×10^{-11} ergs/s/cm^2 over 90% of the sky reveals several low-mass X-ray binaries in the region only. If there is no bright X-ray counterpart for G350.6-4.7, a possibility for the origin of the source is the IC scattering of energetic leptons in a relic PWN.

A young PWN has a characteristic spectral energy distribution with two humps, one in X-rays attributed to synchrotron radiation of very-high energy leptons and another in the gamma-ray range produced by IC scattering of ambient photon fields by energetic leptons (e.g., Gelfand et al. 2009). However, the X-ray emission of evolved (relic) PWN is very low or absent leaving a VHE source with no counterpart.

Although the details of the PWN evolution depend on the associated pulsar and the magnetic field, a typical prediction for the spectral energy distribution of an evolved 24 kyr-PWN taken from Vorster et al. (2013) is shown in Fig. 3 with the measured LAT spectral energy distribution of G350.6-4.7. The model was taken from that calculated for HESS J1507-622 in an ancient PWN scenario and it is scaled-up by a factor of 1.5. This is a peculiar source discovered in a H.E.S.S. Galactic Plane Survey (H.E.S.S. Collaboration et al. 2011), located relatively far from the Galactic plane ($\sim 3°.5$), which has no clear X-ray counterpart. The reader is referred to this work for details on the model parameters. It is expected that the older a PWN becomes the lower its X-ray fluxes are, and the peak of the synchrotron hump is displaced to lower and lower energies while keeping the power-law component in the GeV band hard (Mayer et al. 2012), so this is a plausible scenario for the origin of the high-energy photons although the model in Fig. 3 fails to reproduce the shape of the spectral energy distribution.

Extended gamma-ray sources such as G350.6-4.7 offer an exciting possibility to carry out spatially-resolved spectral modeling with the LAT. This is relevant to understand particle diffusion in some sources interacting with the ambient as well as to probe the local acceleration properties of a source. If the source is nearby as its extension suggests, it could have an impact in the measured electron (or positron) spectrum locally. It then becomes important to constrain its distance. The necessary future studies to unveil the nature of G350.6-4.7 will likely benefit from observations at other wavelengths.

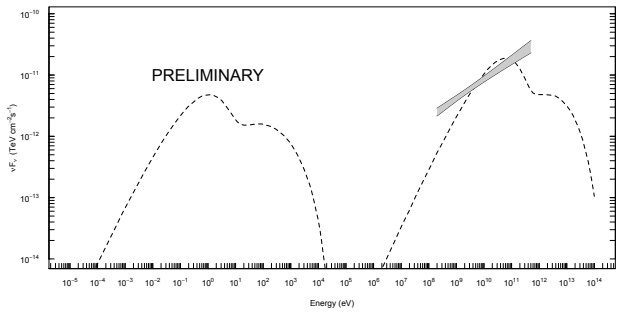

Figure 3. The same data shown in Fig. 2 with a scaled-up relic PWN model (dashed line) for the source HESS J1507-622.

ACKNOWLEDGEMENTS

Financial support from Universidad de Costa Rica is acknowledged. This research has made use of NASA's Astrophysical Data System.

REFERENCES

Abdo A. A., et al., 2009a, ApJ, 701, L123
Abdo A. A., et al., 2009b, ApJ, 706, L1
Abdo A. A., et al., 2010a, ApJS, 187, 460
Abdo A. A., et al., 2010b, ApJ, 710, L92
Abdo A. A., et al., 2011, ApJ, 734, 28
Abdo A. A., et al., 2013, ApJS, 208, 17
Acero F., et al., 2013, ApJ, 773, 77
Acero F., et al., 2015, ApJS, 218, 23
Acero F., et al., 2016, ApJS, 224, 8
Ackermann M., et al., 2013, Science, 339, 807
Ackermann M., et al., 2014a, Science, 345, 554
Ackermann M., et al., 2014b, ApJ, 793, 64
Ackermann M., et al., 2015, ApJ, 810, 14
Ackermann M., et al., 2016, The Astrophysical Journal Supplement Series, 222, 5
Atwood W. B., et al., 2009, ApJ, 697, 1071
Baumgartner W. H., Tueller J., Markwardt C. B., Skinner G. K., Barthelmy S., Mushotzky R. F., Evans P. A., Gehrels N., 2013, ApJS, 207, 19
Bell A. R., 2014, Brazilian Journal of Physics, 44, 415
Blair W. P., Sankrit R., Raymond J. C., 2005, AJ, 129, 2268
Caprioli D., 2012, J. Cosmology Astropart. Phys., 7, 038
Carrigan S., et al., 2013, preprint, (arXiv:1307.4690)
Cioffi D. F., McKee C. F., Bertschinger E., 1988, ApJ, 334, 252
Domainko W. F., 2011, Advances in Space Research, 47, 640
Drury L. O., Aharonian F. A., Voelk H. J., 1994, A&A, 287, 959
Gelfand J. D., Slane P. O., Zhang W., 2009, ApJ, 703, 2051
H.E.S.S. Collaboration et al., 2011, A&A, 525, A45
Katagiri H., et al., 2011, ApJ, 741, 44
Kerr M., et al., 2012, ApJ, 748, L2
Longair M. S., 1994, High energy astrophysics. Volume 2. Stars, the Galaxy and the interstellar medium.
Mattox J. R., et al., 1996, ApJ, 461, 396
Mayer M., Brucker J., Holler M., Jung I., Valerius K., Stegmann C., 2012, preprint, (arXiv:1202.1455)
Pühlhofer G., et al., 2015, preprint, (arXiv:1509.03872)
Slavin J. D., Cox D. P., 1993, ApJ, 417, 187
Su M., Slatyer T. R., Finkbeiner D. P., 2010, ApJ, 724, 1044
Tanaka T., et al., 2011, ApJ, 740, L51
Vorster M. J., Tibolla O., Ferreira S. E. S., Kaufmann S., 2013, ApJ, 773, 139
Yuan Q., Liu S., Fan Z., Bi X., Fryer C. L., 2011, ApJ, 735, 120

This paper has been typeset from a TEX/LATEX file prepared by the author.